Journal of Catalysis **194,** 71–79 (2000)
doi:10.1006/jcat.2000.2915, available online at http://www.idealibrary.com on IDEAL®

Photocatalytic Decomposition of N_2O on Highly Dispersed Ag^+ Ions on TiO_2 Prepared by Photodeposition

Taizo Sano, Nobuaki Negishi, Denis Mas,[1] and Koji Takeuchi

Global Warming Control Department, National Institute for Resources and Environment, 16-3 Onogawa, Tsukuba, Ibaraki 305-8569, Japan

Received December 13, 1999; revised May 1, 2000; accepted May 3, 2000

Nitrous oxide (N_2O) was photocatalytically decomposed on Ag-photodeposited TiO_2 in the presence of methanol vapor. The N_2O decomposition activity of Ag-photodeposited TiO_2 was much higher than that of Ag-loaded TiO_2 prepared by deposition–precipitation or impregnation methods. The difference in the N_2O decomposition activity between the preparation methods was discussed in terms of the surface conditions observed by transmittance electron microscopy and X-ray photoelectron spectroscopy. The N_2O decomposition activity depended on the amount of photodeposited Ag, and the TiO_2 loaded with only 0.16 wt% Ag has revealed the highest level of activity. Highly dispersed Ag^+ ions prepared by photodeposition were effective for the photocatalytic decomposition of N_2O. In the deposition–precipitation or impregnation methods, Ag^+ ions aggregated to form Ag particles and the N_2O decomposition activity of these catalysts showed a low level of efficiency. Nitrogen of N_2O was reduced into N_2 gas, whereas oxygen was released as CO or CO_2 by the reaction with methanol or its derivatives. © 2000 Academic Press

Key Words: **N_2O decomposition; photocatalyst; TiO_2; Ag; photodeposition.**

INTRODUCTION

The techniques for suppression of nitrous oxide (N_2O) emission and removal of N_2O from the atmosphere are strongly desired because of the contributions of N_2O to the global warming and ozone layer depletion. The global warming potential of N_2O is 320 times higher than that of CO_2 (1). As N_2O is kinetically stable but thermodynamically unstable, its lifetime in the atmosphere is long, about 120–150 years (1, 2). Moreover, the N_2O concentration in the atmosphere (ca. 0.31 ppm in 1992) is increasing by 0.25% every year (1, 3).

Photocatalytic decomposition of N_2O is one of the candidate methods for its removal. N_2O can be reduced by the electrons generated by UV irradiation on semiconductor photocatalysts, evolving N_2 (4–7). Since photocatalysts are suitable for treatment of low-concentration gases and are used at room temperature with sunlight as the energy source (8), photocatalytic decomposition has many advantages: the concentration process is not necessary, the reaction condition is mild, and utilization of sunlight leads to energy savings. Several authors have reported photocatalytic decomposition of N_2O using praseodymium catalysts, lanthanoid cation-exchanged mordenites (9), Cu ion-containing ZSM-5 (10), ZnO, Fe_2O_3 (4), and titanium oxide anchored onto porous vycor glass (5). However, either the quantum yields of the photocatalytic decomposition reaction were low or the photocatalysts were activated with short-wavelength photons ($<$300 nm), i.e., not included in the sunlight spectrum.

Titanium dioxide (TiO_2) is well known as a photocatalyst for elimination of environmental pollutants and is a harmless white powder (8, 11–15). The TiO_2 photocatalyst absorbs photons with wavelengths below 400 nm and promotes redox reactions on its surface. The photocatalytic activity of TiO_2 is applied for NO_x removal (12), reduction of CO_2 (13), water splitting (14), decomposition of VOC (8, 15), etc., on a laboratory scale. However, pure TiO_2 does not decompose N_2O even if a reductant is added to the system. In our preliminary experiment, deposition of Pt, Cu, or Ag on TiO_2 as co-catalyst enabled the photocatalytic reaction to proceed in the presence of methanol vapor. Also, Kudo and co-workers reported that TiO_2 with Ag, Cu, Ru, and Pt as co-catalysts photocatalytically decomposes N_2O at room temperature in the presence of methanol and water vapor (6, 7).

In particular, Ag-loaded TiO_2 showed a high level of activity for the photocatalytic decomposition of N_2O, and the addition of Ag to TiO_2 catalyst has been reported to enhance the reduction of NO and thiols (16, 17). However, the states of Ag species (such as oxidation state or dispersion) on TiO_2 surfaces are not well understood. Since the photocatalytic decomposition of N_2O is a heterogeneous process, the surface condition of the photocatalyst should affect the N_2O decomposition activity. Furthermore, the improvement of the catalyst surface would be an important factor in decomposing N_2O efficiently.

---

[1] Permanent address: Laboratoire “Photocatalyse, Catalyse et Environnement,” CNRS UMR “IFoS,” Ecole Centrale de Lyon, BP 163, 69131 Ecully Cedex, France.

0021-9517/00 $35.00

In this paper, Ag-loaded TiO_2 photocatalysts (Ag-TiO_2) for N_2O decomposition were prepared by photodeposition, deposition–precipitation, and impregnation methods. The N_2O decomposition activity of the photocatalysts is discussed, concerning the surface conditions of the photocatalysts determined by X-ray diffractometry (XRD), X-ray photoelectron spectroscopy (XPS), and transmittance electron microscopy (TEM). The mechanism of the photocatalytic process is also discussed.

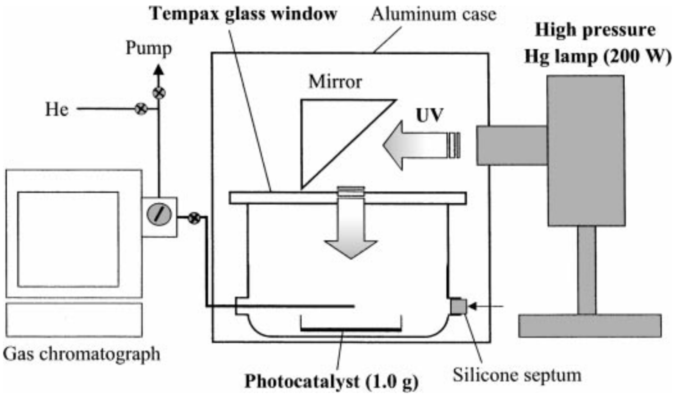

FIG. 1. Experimental set-up for photocatalytic decomposition of N_2O (sample 1.0 g; vessel volume 1830 cm^3; irradiated area 50 cm^2; UV-A irradiance at the sample 1.8 mW cm^{-2}).

METHODS

Preparation of Photocatalysts

The Ag-TiO_2 photocatalysts were synthesized by photodeposition, deposition-precipitation, and impregnation methods (16–21). $AgNO_3$ (analytical grade) and anatase-type TiO_2 (Degussa, P-25) were used. The amount of Ag loaded varyied between 0.01 and 2.0 wt% versus TiO_2.

Photodeposition method. A 3.0-g portion of TiO_2 was dispersed into 75 cm^3 of $AgNO_3$ solution (3.7×10^{-5} to 7.4×10^{-3} mol dm^{-3}). The pH of the suspension was adjusted to 6.3 by addition of KOH solution (0.01–0.1 mol dm^{-3}) while the suspension was stirred vigorously by a magnetic stirrer. The suspension was aged for 15 min at room temperature. Then, 2 cm^3 of methanol was added to the suspension, before being poured into the quartz cell for photodeposition. UV light from a high-pressure Hg lamp (Ushio, USH-500D, 500 W) was irradiated to the suspension through a longpass filter (cut-off wavelength 295 nm) for 30 min while N_2 gas was passed through the suspension (photodeposition process). The product was collected by the aid of centrifugation, washed with distilled water four times, and then dried in air at 383 K for 12 h.

Impregnation method. TiO_2 was dispersed into $AgNO_3$ solution containing the required amount of Ag and dried in air at 383 K. The precursor was heat-treated in air at 773 K for 3 h to form Ag-TiO_2.

Deposition–precipitation method. TiO_2 was dispersed in $AgNO_3$ solution containing the required amount of Ag. The pH of the suspension was adjusted to 6.8 by adding KOH solution (0.01–0.1 mol dm^{-3}) to precipitate Ag^+ ions on TiO_2. The precipitate was collected by the aid of centrifugation, washed with distilled water four times, and then dried in air at 383 K for 12 h. The precipitate was heat-treated in air at 473 or 573 K for 6 h to obtain Ag-TiO_2 catalysts. The activity of the former (473 K heat treatment) was 20% lower than that of the latter (573 K heat treatment). Thus, only the sample heat-treated at 573 K was used in the present paper.

The solid phases were identified by XRD with Cu$K\alpha$ radiation (Rigaku, Model RU-300), XPS with Al$K\alpha$ radiation (Fisons Instruments, Escalab220i-XL), and TEM (Philips, CM30). The amount of Ag deposited was determined by X-ray fluorescence analysis (XRF; Philips, PW2404) and inductively coupled plasma spectrometry (ICP; Shimadzu, ICPS7000).

Photocatalytic Decomposition of N_2O

The experimental set-up is schematically shown in Fig. 1. A 1.0-g portion of the Ag-TiO_2 photocatalyst was dispersed on a laboratory glass dish (8 cm in diameter) that was placed in the reaction vessel (1.83 dm^3) with a cover window of Tempax glass (8 mm in thickness, cut-off wavelength of 300 nm). After the reaction vessel was filled with He to the atmospheric pressure, N_2O was injected into the vessel through a silicone septum with a syringe. In the study of the effect of methanol or water vapor, liquid methanol or water was also injected through the septum to be vaporized. The temperature at the center of the sample was monitored with a thermocouple. No significant increase in the temperature was observed during the photoreactions. During the photocatalytic decomposition of N_2O, the photocatalyst was irradiated with UV light from a high-pressure mercury lamp (Ushio, USH-102D, 200 W) through the Tempax glass window. The UV irradiance at the sample surface was approximately 1.8 mW cm^{-2}. Gases in the reaction vessel were analyzed using a gas chromatograph (Shimadzu, GC8A) and gas chromatograph–mass spectrometry (GC-MS) (Hewlett Packard, GC-MS5972A).

RESULTS AND DISCUSSION

Characterization of the Photocatalysts

The photocatalysts prepared by photodeposition, deposition–precipitation, and impregnation methods are abbreviated as PDx, DPx, and IMx, where x denotes the weight percentage of loaded Ag versus TiO_2, which was determined by XRF. The typical photocatalysts

TABLE 1

Photocatalysts Prepared and Studied

Sample	Method	Ag (wt% against TiO_2) In suspension[a]	Ag (wt% against TiO_2) On TiO_2[b]	Temperature[c] (K)	Crystallite size[d] (nm)
TiO_2		0	0	383	25
PD1.60	Photodeposition	2.00	1.6	383	26
PD0.16	Photodeposition	0.20	0.16	383	24
DP0.67	Deposition–precipitation	1.00	0.67	573	25
DP0.11	Deposition–precipitation	0.10	0.11	573	25
IM0.90	Impregnation	1.00	0.90	773	24
IM0.10	Impregnation	0.10	0.10	773	25

[a] Amount of Ag contained in the preparation suspension.
[b] Amount of Ag loaded on TiO_2 determined by XRF.
[c] Highest temperature of heat treatment.
[d] Crystallite size of TiO_2 (anatase) calculated from XRD pattern.

prepared are listed in Table 1 along with their preparation conditions. For the impregnation method, the amounts of Ag loaded were identical with the amount of Ag in the preparation suspension. For the deposition–precipitation and photodeposition methods, the amount of Ag loaded was equal to or lower than that contained in the preparation suspension. This indicates that the Ag^+ ion in the preparation suspension was not completely deposited on TiO_2. The relation between the amounts of Ag in the preparation suspension and on the TiO_2 photocatalyst prepared by the photodeposition method is shown in Fig. 2. The difference between the amounts of Ag in suspension and on TiO_2 increased with increasing amounts of Ag in suspension. In the present study, UV-irradiation time for photodeposition was set to be constant (30 min), regardless of the Ag content. It is considered that the UV-irradiation time was short for the photodeposition of a larger amount of Ag and that all of Ag^+ ions in the suspension were not photodeposited.

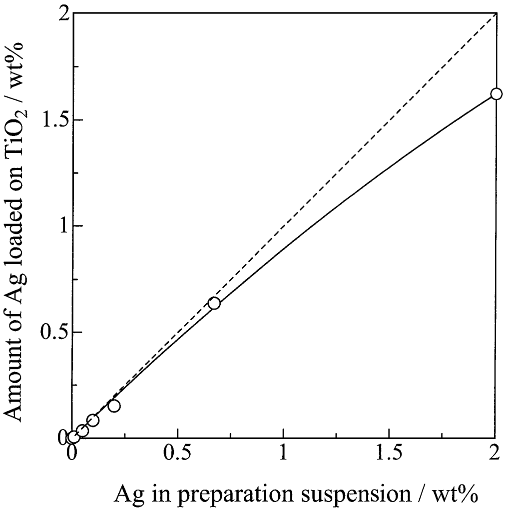

FIG. 2. Relation between the amount of Ag contained in the preparation suspension and the amount loaded on TiO_2.

In the XRD patterns of all photocatalysts, only the peaks of TiO_2, anatase and rutile, appeared but no peaks of Ag or Ag-related compounds were detected. This indicates that the Ag was loaded in the state of ions or small nondetectable particles. The *d*-spacing of the anatase or rutile in the photocatalysts was identical to that of the raw material. The crystallite sizes of the anatase in the photocatalysts were determined from the half-width of the 200 plane of anatase crystal using the Scherrer formula ($t = 0.9\lambda/B\cos\theta$) and are listed in Table 1. The crystallite sizes of all the photocatalysts were similar (24–26 nm) and were not dependent on the preparation method. This indicates that sintering of TiO_2 crystallite does not proceed significantly at temperatures below 773 K. Therefore, the specific surface areas of the photocatalysts are consistent with that of the initial material (P-25, $\sim$50 $m^2\ g^{-1}$).

The characteristics of Ag deposited on the photocatalysts were analyzed by XPS. Figure 3 shows the Ag 3*d* spectra for the photocatalysts. The peaks at around 367 eV (Ag $3d_{5/2}$) in the XPS spectra are slightly broadened and are considered to be the sum of multiple peaks. Figure 4a shows the results of curve fitting for PD1.6 by a complex of Lorentzian and Gaussian curves. The spectra for other samples were also divided into two peaks, *a* (368.2 eV) and *b* (367.6 eV). The information for the curves is listed in Table 2. The resolved peaks *a* and *b* can be attributed to the peaks of metal Ag and Ag^+ (Ag_2O), respectively (22, 23). In all the spectra, the peak for Ag^+ ions is larger than the peak for metal Ag. During the preparation process by photodeposition, Ag^+ ions in the suspension were reduced on the TiO_2 surface and were deposited as metal Ag (21). However, a part of photodeposited Ag could have been oxidized to Ag^+ in air after preparation. In the deposition–precipitation and impregnation methods, Ag species deposited on the photocatalysts were partially reduced to metal Ag during the heat

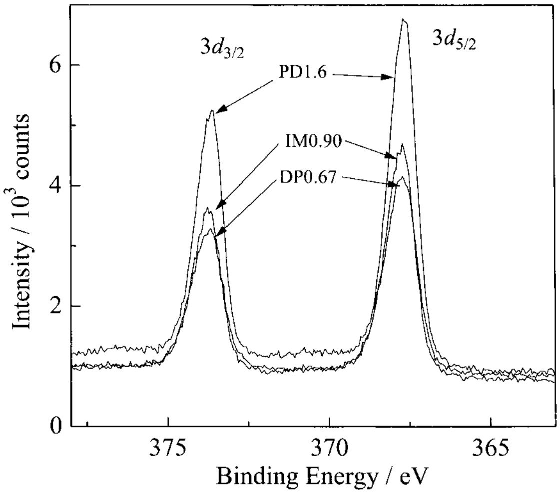

FIG. 3. XPS spectra of the Ag-TiO_2 photocatalysts prepared by photodeposition, deposition-precipitation and impregnation methods.

TABLE 2

Results of XPS for Ag-TiO_2 Photocatalysts

	Binding energy (eV)		Relative intensity (arbitrary unit)			
Sample	Peak *a*	Peak *b*	Peak *a*	Peak *b*	$b/a+b$	Total
PD1.60	368.2	367.6	1.63	7.45	0.72	9.08
PD0.16	368.2	367.6	0.23	0.77	0.77	1.00
DP0.67	368.2	367.6	2.16	4.18	0.66	6.34
DP0.11	—	367.5	—	0.10	—	0.10
IM0.90	368.2	367.7	2.28	5.24	0.70	7.52
IM0.10	368.2	367.7	0.04	0.33	0.89	0.37

treatment (573 K for deposition–precipitation and 773 K for impregnation methods), and both metal Ag and Ag^+ ions were detected.

The integrated intensity of the Ag $3d_{5/2}$ peak for PD1.6 is 9 times higher than that for PD0.16 (Table 2). This roughly coincides with the ratio of loaded Ag amounts (10 times) determined by XRF. On the other hand, the intensity for DP0.11 or IM0.10 is much smaller than that for DP0.67 or IM0.90, respectively, even if the amounts of Ag deposited are considered. This suggests that the amount of Ag existing on the surface was different from the amount of Ag loaded. This may be due to the diffusion of Ag from the TiO_2 surface to the interior during the heat treatment.

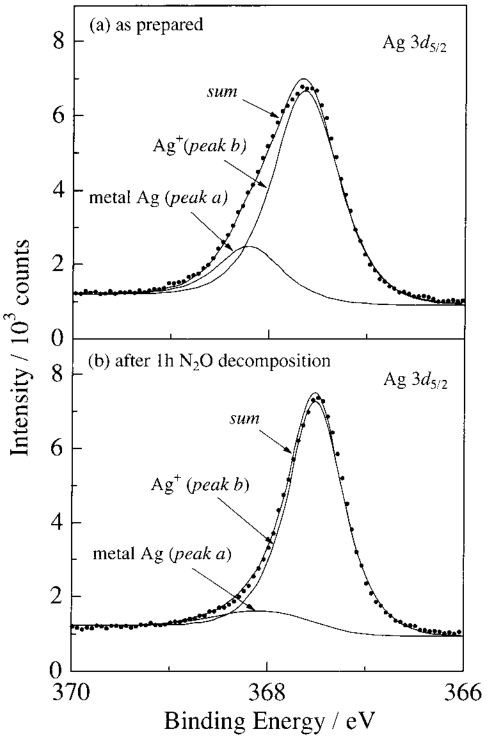

FIG. 4. XPS spectra of Ag-photodeposited TiO_2 (PD1.6) as prepared (a) and after the photocatalytic decomposition of N_2O for 1 h in the presence of methanol and water vapor (b).

Figures 5a–5f show the TEM photographs of the photocatalysts. The crystallite sizes of all photocatalysts observed by TEM are approximately identical with the values determined by XRD. Figure 5a is the TEM photograph of PD0.16. No significant changes in surface conditions are observed, and the photograph is almost similar to that of the initial material (TiO_2, P-25). In the photograph for PD1.6 (Fig. 5b), the small particles of Ag with a diameter of 1–2 nm are noticeable. They might be formed on the surface by aggregation of Ag in the photodeposition process when a large amount of Ag is photodeposited. The aggregation of Ag could be probably explained by both the high Ag^+ concentration and the large absolute amount of Ag^+ in the preparation suspension. The aggregation of Ag is more obvious on the photocatalysts prepared by deposition–precipitation and impregnation methods. In both preparation methods, only 0.1 wt% of loaded Ag forms the Ag particles (Fig. 5c for DP0.11 and Fig. 5e for IM0.10).

Based on the results of XPS, a larger amount of Ag exists on the surface of PD0.16 than on the surface of DP0.11 or IM0.10. However, the aggregation of Ag is not confirmed on PD0.16. Therefore, Ag species on PD0.16 are highly dispersed, compared with DP0.11 or IM0.10. The number of Ag particles observed on PD1.6 is not so different from that on DP0.11 or DP0.67, while the Ag peak intensity in XPS spectrum for the PD1.6 is larger than that of DP0.11 or DP0.67. This suggests that a large proportion of the Ag species was well dispersed on PD1.6 and a small proportion of the Ag species aggregated on the surface.

A rough surface is observed for IM0.10 and IM0.90 (Figs. 5e and 5f). This may be due to the heat treatment at higher temperature (773 K in air), which would promote the reaction of Ag species with the TiO_2 surface. Although the amounts of Ag loaded on IM0.10 and IM0.90 are different, the degrees of roughness are not so different. This

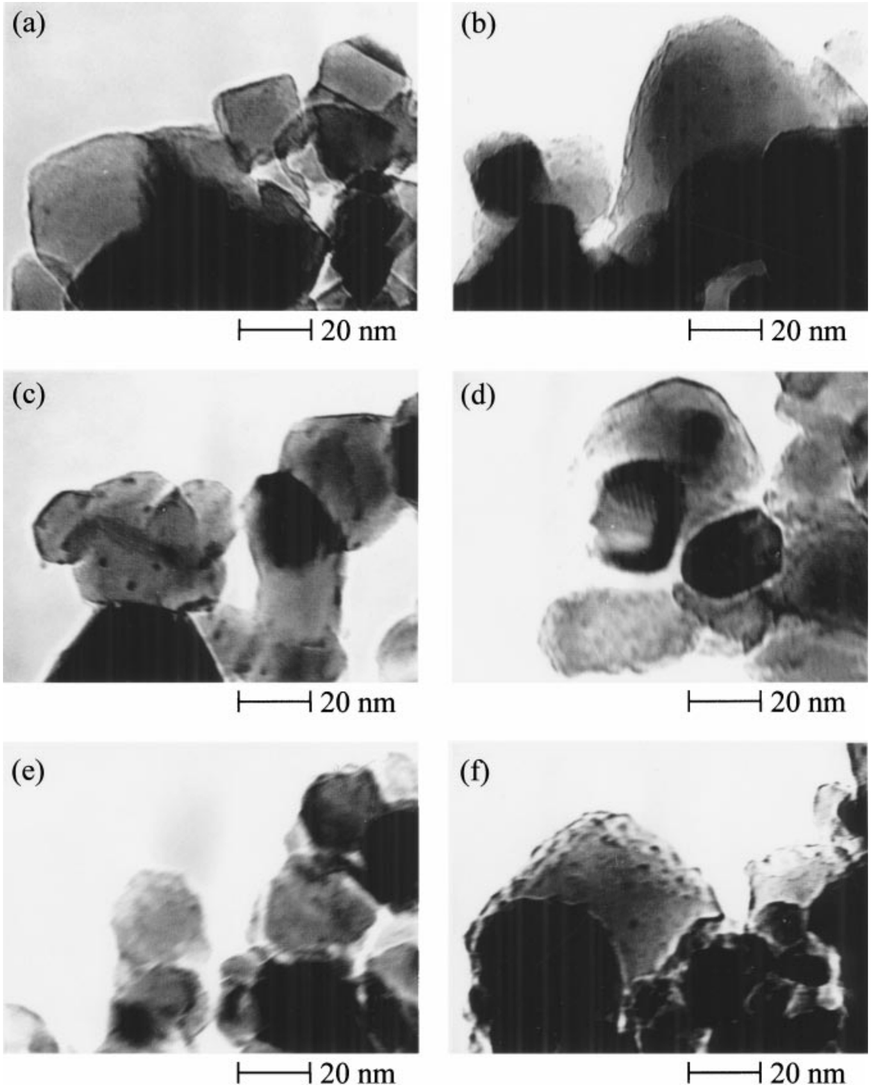

FIG. 5. TEM photographs of Ag-TiO_2 prepared by (a,b) photodeposition, (c,d) deposition–precipitation, and (e,f) impregnation methods. (a) PD0.16, (b) PD1.60, (c) DP0.11, (d) DP0.65, (e) IM0.10, and (f) IM0.90.

suggests that the bumps on the surface are not Ag particles themselves. The bumps may be formed in the course of Ag^+ migration into the TiO_2 surface layer during the heat treatment. In the photodeposition method, a heat treatment at high temperature was not necessary and the surface of the photocatalysts retained its original shape.

IM0.11 and IM0.90 were dispersed into 1.0 mol dm^{-3} HNO_3 solution, and the amount of Ag dissolved was determined by ICP spectrometry. Only 0.024 and 0.443 wt% of Ag was detected for IM0.11 and IM0.90, respectively. Since these values are much smaller than the amounts of Ag determined by XRF (0.11 and 0.90 wt%), the other part of Ag may combine strongly with TiO_2 and not dissolve in HNO_3 solution. It is considered that Ag^+ ions migrated into the TiO_2 and that Ag-TiO_2 compounds were formed during the heat treatment at 773 K. On the other hand, the major part (>90%) of Ag on the photocatalysts prepared by the photodeposition method was dissolved in HNO_3 solution. This suggests that Ag existed on the outermost layer of the photocatalyst and did not bind strongly with TiO_2.

N_2O Decomposition Activities of Ag-TiO_2 Photocatalysts

Figure 6 shows a typical profile for the photocatalytic decomposition of N_2O by Ag-photodeposited TiO_2 (Ag 0.64 wt%) in the presence of methanol (0.63 kPa) and water vapor (1.4 kPa). When the photocatalyst was not irradiated by UV light, N_2O was not decomposed. After the beginning of UV irradiation at time 0, the partial pressure of N_2O decreased from 0.14 to 0.04 kPa within 2 h. Then, additional N_2O was injected into a reaction vessel and the N_2O decomposition was continued while methanol was added

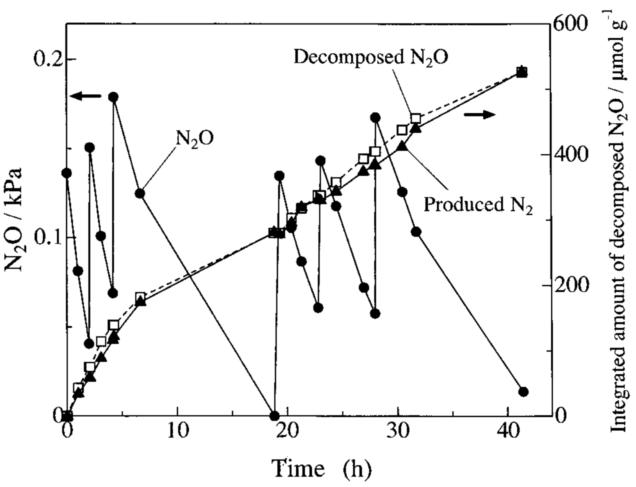

FIG. 6. N_2O decomposition with Ag-photodeposited TiO_2 (Ag 0.64 wt%) under UV irradiation (initial pressure of N_2O 0.14 kPa; MeOH 0.63 kPa; H_2O 1.4 kPa).

occasionally. The Ag-photodeposited TiO_2 lowered the partial pressure of N_2O below 1 Pa (at 18 h). The integrated amount of N_2O decomposed and the amount of N_2 evolved (shown in Fig. 6) were almost equal. This indicates that N_2O was decomposed into N_2. Oxygen was not produced while a very small amount of H_2 gas was detected. The gas phase contained 100 μmol of CO_2 and 32 μmol of CO after a 42-h reaction. These results suggest that the oxygen atom of N_2O was released as CO, CO_2, and H_2O by the reaction with methanol vapor.

The formations of CO_2 and CO are represented by the following stoichiometric equations:

$$2N_2O + CH_3OH \rightarrow 2N_2 + CO + 2H_2O, \qquad [1]$$

$$3N_2O + CH_3OH \rightarrow 3N_2 + CO_2 + 2H_2O. \qquad [2]$$

Based on the amounts of CO and CO_2 produced, the amount of N_2O decomposed can be estimated to be 364 μmol, which is smaller than the amount of N_2O actually decomposed (520 μmol). This suggests that a part of the oxygen atom of decomposed N_2O was released as other compounds. The reaction gas mixture was further analyzed by GC-MS. In the gas phase, acetaldehyde, methyl formate, dimethoxymethane, methyl acetate, acetic acid, ethyl acetate, and small amounts of other organic compounds were detected along with unchanged methanol. These organic compounds were produced by the partial oxidation of methanol with oxygen atoms of N_2O. When the addition of methanol was stopped, the concentrations of these organic compounds began to decrease and the CO_2 concentration increased. These results suggest that the partial oxidation of methanol was faster than the complete oxidation of the detected intermediate organic compounds. The depression of the production of intermediate compounds could be realized by controlling the concentration of methanol vapor. Neither NO nor NO_2 was detected in the reaction gas mixture.

The photocatalysts prepared by the photodeposition method decomposed N_2O more rapidly than those prepared by the deposition–precipitation and impregnation methods. Figure 7a shows the photocatalytic decomposition of N_2O by Ag-TiO_2 with low Ag content in the presence of methanol (0.63 kPa) and water vapor (1.4 kPa). The N_2O decomposition rate with PD0.16 was about 12 times higher than that with DP0.11 or IM0.10. Based on the XPS analysis, the amount of Ag present on the surface of the photocatalyst prepared by the photodeposition method is 10 times larger than in the case of photocatalysts prepared by the deposition–precipitation method. The difference in the amount of Ag effective for N_2O decomposition may be one of the factors responsible for the higher activity of PD0.16. However, the difference between the

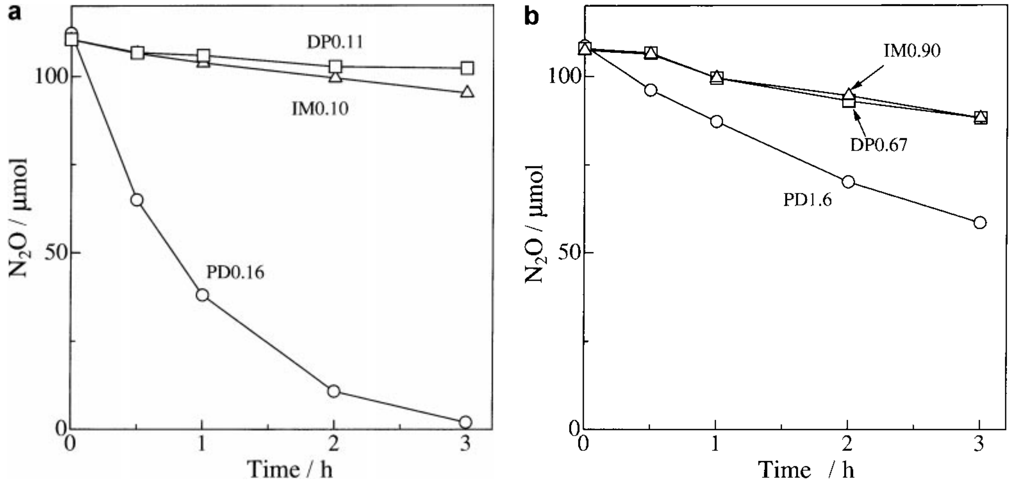

FIG. 7. Decomposition of N_2O by Ag-TiO_2 photocatalysts; (a) low Ag content and (b) high Ag content (initial pressure of N_2O 0.14 kPa; MeOH 0.63 kPa; H_2O 1.4 kPa). (○) Photodeposition, (□) deposition–precipitation, and (△) impregnation methods.

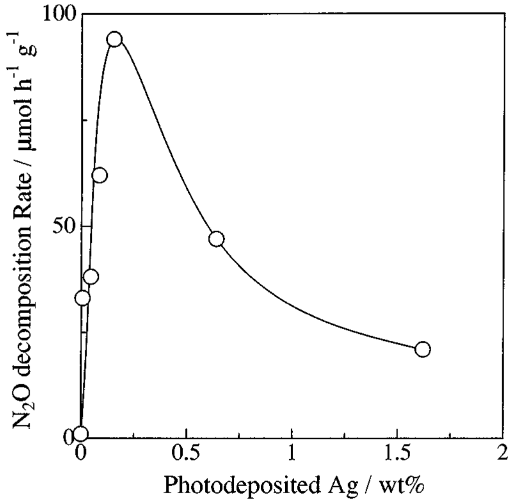

FIG. 8. Effect of the amount of photodeposited Ag on N_2O decomposition rate (initial pressure of N_2O 0.14 kPa; MeOH 0.63 kPa; H_2O 1.4 kPa).

decomposition rates of PD0.16 and IM0.10 is much larger than the difference between the amounts of Ag on PD0.16 and IM0.10 determined by XPS. Therefore, the N_2O decomposition rates may be also due to the states of Ag species on the TiO_2 surface. The dispersion of Ag on PD0.16 seems to be higher than that on DP0.11 or IM0.10, since Ag did not aggregate on PD0.16 while Ag aggregated on DP0.11 and IM0.10 as shown in TEM photographs. The high dispersion of Ag on PD0.16 may enhance the adsorption of N_2O and lead to a higher activity. For the photocatalysts with larger Ag content (Fig. 7b), the difference between the photocatalytic activities of PD1.6 and DP0.67 (or IM0.90) was lower than the difference between those of PD0.16 and DP0.11 (or IM0.10) (Fig. 7b). As the Ag aggregation occurred on PD1.6 similarly to DP0.67 or IM1.0, the dispersion of Ag on PD1.6 may be lower than that on PD0.16, decreasing the photocatalytic activity of PD1.6.

In the photodeposition method, Ag was deposited selectively on the reduction sites of the TiO_2 surface (19). On the other hand, Ag was deposited randomly in the case of the deposition–precipitation or impregnation methods. It can be assumed that the selective deposition on reduction sites is one of the reasons for the higher activity of Ag-photodeposited TiO_2. Since N_2O has been adsorbed and reduced on Ag during the photocatalytic reaction, Ag on the reduction site, where electrons are sufficiently provided, would be a highly active site for N_2O reduction.

The effect of the amount of photodeposited Ag on the N_2O decomposition rate is shown in Fig. 8. The decomposition rate was calculated from the amount of N_2O decomposed during the initial 30 min of UV irradiation. The TiO_2 without Ag deposition did not decompose N_2O at all; however, the TiO_2 with photodeposited Ag decomposed N_2O even when only 0.007 wt% of Ag had been photodeposited. In the case where the amount of photodeposited Ag was lower than 0.16 wt%, the N_2O decomposition rate increased with the amount of Ag. This suggests that the photodeposited Ag is the active site for the photocatalytic decomposition of N_2O. The maximum decomposition rate (94 μmol h^{-1} g^{-1}) was obtained with 0.16 wt% Ag-deposited TiO_2 (PD0.16), where the apparent quantum yield was 9.4%. When the amount of Ag was larger than 0.16 wt%, the N_2O decomposition rate decreased with an increasing amount of Ag. This decreasing activity may be due to a diminution of the dispersion of Ag on the TiO_2 surface. As described above, the aggregation of Ag was observed on PD1.6 by TEM, while it was not observed on PD0.16. The aggregation seems to occur when the amount of Ag is over 0.16 wt%, and this may decrease the number of N_2O adsorption sites and thus decrease the photocatalytic decomposition activity, as shown in Fig. 8.

Mechanism of N_2O Decomposition on Ag-TiO_2 Photocatalysts

The oxidation state of Ag on Ag-photodeposited TiO_2 after N_2O decomposition for 1 h in the presence of methanol and water vapor was analyzed by XPS. The spectrum for PD1.6 (Fig. 4b) is similar to that for PD0.16 except for the absolute intensity range. The peak of metal Ag (peak *a*, 368.2 eV) was small, and the large part of Ag existed as Ag^+ ions of Ag_2O (peak *b*, 367.6 eV). It is considered that the metal Ag in PD1.6 as prepared was oxidized into Ag^+ ions in the initial stage of the photocatalytic N_2O decomposition. The N_2O decomposition activity did not decrease despite the decrease in the amount of metal Ag. This result suggests that Ag^+ ions participated in the photoreaction.

The effect of H_2 reduction of Ag-loaded TiO_2 on N_2O decomposition activity was investigated. One gram of photocatalyst was reduced under a H_2 gas stream (50 cm^3 min^{-1}) at 373 or 573 K for 30 min and was transferred into the reaction vessel. N_2O decomposition activity was measured in the presence of methanol (0.63 kPa) and water vapor (1.4 kPa). As shown in Table 3, H_2 reduction at 373 K on

TABLE 3

Effect of H_2 Reduction of Ag-Loaded TiO_2 on Photocatalytic Activity

Sample	H_2 reduction temperature	N_2O decomposition rate[a] (μmol h^{-1} g^{-1})
PD0.085	—	40.8
PD0.085	373 K	22.2
DP0.67	—	8.3
DP0.67	373 K	10.5
DP0.67	573 K	4.2
IM0.90	—	7.9
IM0.90	373 K	12.4

[a] N_2O decomposition rate calculated from the amount of N_2O decomposed during the initial 1 h.

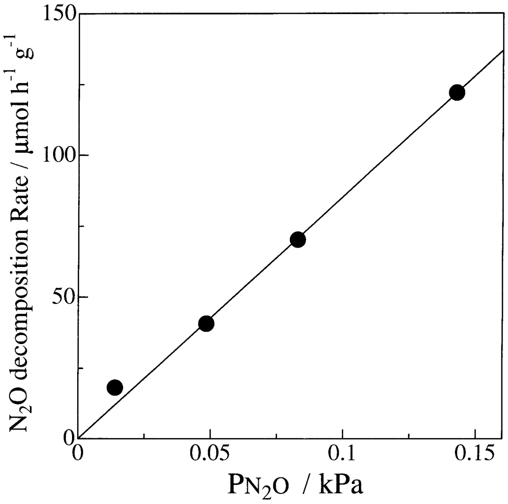

FIG. 9. Increase in N_2O decomposition rate with partial pressure of N_2O. Sample is Ag-photodeposited TiO_2 (PD0.16) (initial pressure of MeOH 0.63 kPa; H_2O 1.4 kPa).

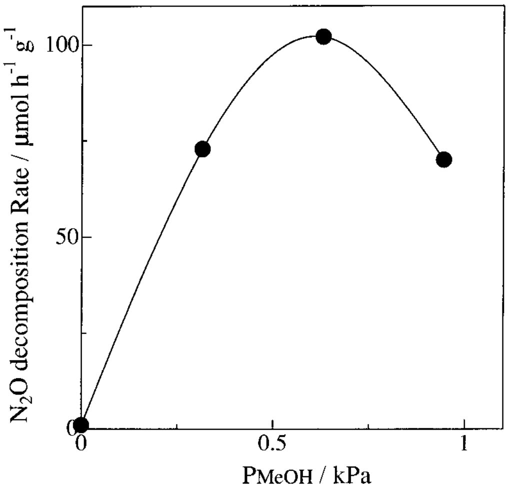

FIG. 10. Effect of partial pressure of methanol on N_2O decomposition rate with Ag-photodeposited TiO_2 (PD0.16). P_{N_2O} was 0.14 kPa, H_2O was not added.

DP0.67 or IM0.90 increased the activity by 20–50%. However, further reduction at 573 K on DP0.67 lowered the activity. These results suggest that a partially reduced Ag_2O phase possessed the high activity for N_2O decomposition and that the activity of metal Ag, which was formed by H_2 reduction at 573 K, was lower than the activity of Ag_2O. The activity of PD0.085 reduced at 373 K was lower than that of PD0.085 as prepared. This suggests that Ag was deposited in the form of partially reduced Ag_2O by the photodeposition method. H_2 reduction at 373 K on PD0.085 may form metal Ag with lower activity.

Figure 9 shows the relation between the partial pressure of N_2O (P_{N_2O}) and N_2O decomposition rate by PD0.16 photocatalyst. The decomposition rate was determined from the tangent of the curve that was fitted to the N_2O decay shown in Fig. 6a. The decomposition rate increased linearly with increasing N_2O partial pressure. Figure 10 shows the relation between the partial pressure of methanol (P_{MeOH}) and N_2O decomposition rate. In the absence of methanol in the reaction vessel, the photocatalytic decomposition of N_2O did not occur on Ag-photodeposited TiO_2. The decomposition rate increased with P_{MeOH} ($0 < P_{MeOH} < 0.63$ kPa). These results suggest that the decomposition rate is determined by the amounts of N_2O and methanol adsorbed on the photocatalyst surface. The photocatalytic decomposition of N_2O was depressed if a higher pressure of methanol ($P_{MeOH} > 0.63$ kPa) was applied. It could be assumed that methanol is adsorbed on both the oxidation sites (TiO_2) and the reduction sites (Ag^+ sites), and this adsorption on the latter sites prevents N_2O from adsorbing, resulting in the depression of the N_2O decomposition.

The effect of water vapor on the photocatalytic decomposition of N_2O was investigated for PD0.085 (Fig. 11). The N_2O decomposition rate decreased with increasing water vapor pressure (P_{H_2O}). This result is opposite to the effect of P_{H_2O} on the photocatalytic decomposition of N_2O with Pt-loaded TiO_2 photocatalyst (7). In the decomposition with Pt-TiO_2, N_2O was not decomposed in the absence of water, and it was inferred that N_2O was reduced by atomic hydrogen formed by the photoreduction of water on a platinum surface. In the N_2O decomposition by Ag-photodeposited TiO_2, the above-mentioned mechanism was not effective. On the contrary, the adsorption of H_2O on Ag-photodeposited TiO_2 depressed the adsorption of N_2O and methanol and thus decreased the N_2O decomposition rate.

The photocatalytic decomposition of N_2O on Ag-TiO_2 is considered to be initiated by the formation of electrons

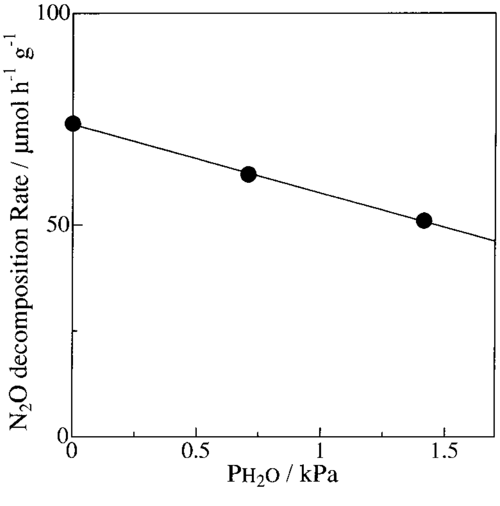

FIG. 11. Effect of partial pressure of H_2O on N_2O decomposition rate with Ag-photodeposited TiO_2 (PD0.085) (initial pressure of N_2O 0.14 kPa; MeOH 0.63 kPa).

(e^-) and holes (h^+) resulting from the photon absorption by TiO_2 (5–8, 11). The electrons transferred from TiO_2 via Ag^+ reduce N_2O adsorbed on Ag^+, and the holes oxidize methanol into CO_2 and H_2O (6). The reduction of N_2O to N_2 could be described in three ways: first, through the reaction of N_2O^- with methanol (Eqs. [4] and [5]); second, through the formation of Ag–O (Eqs. [4], [6], and [7]); and third, through the reaction of O^- with methanol (Eqs. [8] and [9]),

$$TiO_2 + h\nu \rightarrow h^+ + e^-, \qquad [3]$$

$$N_2O_{(ads)} + e^- \rightarrow N_2O^-_{(ads)}, \qquad [4]$$

$$N_2O^-_{(ads)} + \tfrac{1}{3}CH_3OH_{(ads)} + h^+ \rightarrow N_2 + \tfrac{1}{3}CO_2 + \tfrac{2}{3}H_2O, \qquad [5]$$

$$N_2O^-_{(ads)} + Ag^+ \rightarrow N_2 + Ag\text{–}O, \qquad [6]$$

$$Ag\text{–}O + \tfrac{1}{3}CH_3OH_{(ads)} + h^+ \rightarrow Ag^+ + \tfrac{1}{3}CO_2 + \tfrac{2}{3}H_2O, \qquad [7]$$

$$N_2O_{(ads)} + e^- \rightarrow N_2 + O^-_{(ads)}, \qquad [8]$$

$$O^-_{(ads)} + \tfrac{1}{3}CH_3OH_{(ads)} + h^+ \rightarrow \tfrac{1}{3}CO_2 + \tfrac{2}{3}H_2O, \qquad [9]$$

where $N_2O_{(ads)}$, $N_2O^-_{(ads)}$, $CH_3OH_{(ads)}$, and $O^-_{(ads)}$ are chemical species adsorbed on the photocatalyst surface. Ag–O denotes the Ag^+ combined with an extra oxygen. In the photocatalytic decomposition of N_2O by titanium oxide anchored onto porous vycor glass (in the absence of Ag^+ ions), the formation of N_2O^- has been confirmed by electron spin resonance (ESR) (5). Also, in the thermal catalytic decomposition on ZnO, the formation of N_2O^- has been reported (24). Since TiO_2 and ZnO do not have large nonstoichiometric composition, they could not retain extra oxide ions on their surface. On the other hand, Ag-TiO_2 includes Ag^+ ions on its surface, which may be oxidized to form Ag^{2+} when accepting an oxide ion from N_2O. This suggests that the formation of Ag–O and $O^-_{(ads)}$ on Ag-TiO_2 is possible. Therefore, the reaction pathway through Ag–O or $O^-_{(ads)}$ is not rejected in the present study. The analyses of radical species or molecules adsorbed on the photocatalyst by ESR and Fourier transform infrared spectroscopy would clarify the pathway. We will describe the results of those analyses elsewhere.

CONCLUSION

The N_2O decomposition activity of Ag-photodeposited TiO_2 was much higher than that of Ag-TiO_2 prepared by deposition–precipitation or impregnation methods. The N_2O decomposition activity depends on the amount of photodeposited Ag and the state of the Ag species. The highest activity was obtained for 0.16 wt% Ag-photodeposited TiO_2 (PD0.16). The TEM images and XPS spectra suggest that photodeposited Ag species were highly dispersed without aggregation, while aggregation occurred on the other photocatalysts. The photocatalytic decomposition rate of N_2O increased with increasing P_{N_2O} or P_{MeOH}, whereas it decreased with increasing P_{H_2O}. The decomposition rate can be determined by the amounts of N_2O and methanol adsorbed on the photocatalyst surface. Highly dispersed Ag^+ on PD0.16 probably enhanced the adsorption and decomposition of N_2O.

REFERENCES

1. Kisho-cho (Ed.), “Chikyu Ondanka Report 1994” Printing Bureau, Ministry of Finance, Tokyo, 1995.
2. Berkner, L. V., and Marshall, L. C., *in* “The Origin and Evolution of Atmospheres and Oceans” (P. J. Brancazio and A. G. W. Cameron, Eds.), p. 102. Wiley, New York, 1964.
3. Perman, G. I., Etheridge, D., Silva, F., and Fraser, P. J., *Nature* **320**, 248 (1986).
4. Cunningham, J., Kelly, J. J., and Penny, A. L., *J. Phys. Chem.* **75**, 617 (1971).
5. Anpo, M., Aikawa, N., Kubokawa, Y., Che, M., Louis, C., and Giamello, E., *J. Phys. Chem.* **89**, 5017 (1985).
6. Kudo, A., and Nagayoshi, H., *Catal. Lett.* **52**, 109 (1998).
7. Kudo, A., and Sakata, T., *Chem. Lett.*, 2381 (1992).
8. Hoffmann, M. R., Martin, S. T., Choi, W., and Bahnemann, D. W., *Chem. Rev.* **95**, 69 (1995).
9. Ebitani, K., Hirano, Y., and Morikawa, A., *J. Catal.* **157**, 262 (1995).
10. Ebitani, K., Morokuma, M., Kim, J. H., and Morikawa, A., *J. Chem. Soc. Faraday Trans.* **90**, 377 (1994).
11. Linsebigler, A. L., Lu, G., and Yates, J. T., *Chem. Rev.* **95**, 735 (1995).
12. Ibusuki, T., and Takeuchi, K., *J. Mol. Catal.* **88**, 93 (1994).
13. Ishitani, O., Inoue, C., Suzuki, Y., and Ibusuki, T., *J. Photochem. Photobiol. A Chem.* **72**, 269 (1993).
14. Yamaguti, K., and Sato, S., *J. Chem. Soc. Faraday Trans. I* **81**, 1237 (1985).
15. Negishi, N., Iyoda, T., Hashimoto, K., and Fujishima, A., *Chem. Lett.*, 841 (1995).
16. Haneda, M., Kintaichi, Y., Inaba, M., and Hamada, H., *Bull. Chem. Soc. Jpn.* **70**, 499 (1997).
17. Tada, H., Teranichi, K., Inubushi, Y., and Ito, S., *Chem. Commun.*, 2345 (1998).
18. Sclafani, A., Mozzanega, M. N., and Herrmann, J. M., *J. Catal.* **168**, 117 (1997).
19. Bamwenda, G. R., Tsubota, S., Nakamura, T., and Haruta, M., *J. Photochem. Photobio. A Chem.* **89**, 177 (1995).
20. Schwarz, J. A., Contescu, C., and Contescu, A., *Chem. Rev.* **95**, 477 (1995).
21. Nishimoto, S., Ohtani, B., Kajiwara, H., and Kagiya, T., *J. Chem. Soc. Faraday Trans. I* **79**, 2685 (1983).
22. Wangner, C. D., *in* “Practical Surface Analysis” (D. Briggs and M. P. Seah, Eds.), 2nd ed., Vol. 1, p. 595. Wiley, New York, 1990.
23. Moulder, J. F., Sickle, W. F., Sobol, P. E., and Bomben, K. D., “Handbook of X-ray Photoelectron Spectroscopy,” 2nd ed. Perkin–Elmer, Palo Alto, CA, 1992.
24. Tanaka, K., and Blyholder, G., *J. Phys. Chem.* **75**, 1037 (1971).